This paper is part of the following report:

TITLE: Annual Research Briefs - 2003 [Center for Turbulence Research]

To order the complete compilation report, use: ADA420749

The component part is provided here to allow users access to individually authored sections
of proceedings, annals, symposia, etc. However, the component should be considered within
the context of the overall compilation report and not as a stand-alone technical report.

The following component part numbers comprise the compilation report:
ADP014788 thru ADP014827

RANS simulation of the separated flow over a bump with active control

By Gianluca Iaccarino, Claudio Marongiu†,
Pietro Catalano†, Marcello Amato†

1. Introduction and motivations

Active Flow Control (AFC) is an attractive technique to increase the aerodynamic efficiency of lifting and control surfaces. The working principle is to use localized suction or injection to modify the characteristics of the boundary layer flow near regions of separation, thus limiting the associated losses. The effect of steady suction or blowing has been studied in great detail in the past (see Braslow (1999) for a comprehensive review), especially with reference to high-lift configurations. The major limitation to the applicability of conventional AFC devices is the need to provide or discharge a constant supply of flow for blowing or suction, respectively, which requires complicated piping, additional energy supply, and causes efficiency losses. In the last decade, a new AFC device, namely the synthetic jet actuator, has been introduced, which eliminates most of these drawbacks. In this system the net mass flow is zero, because a membrane within a small cavity produces blowing and suction alternatively. The performance of synthetic jets appear to be extremely encouraging, but most of the experimental analysis and numerical studies are performed at low Reynolds number. The current focus is on the application of such devices to turbulent flows especially in the aeronautical industry.

The fluid mechanics of synthetic jets at low Reynolds numbers is well understood (Glezer & Amitay 2002) and their difference with respect to conventional (continuous) jet has been elucidated experimentally (Smith & Swift 2003). In particular, it has been shown that the vortex shedding behind a circular cylinder can be completely suppressed in the laminar regime (Glezer & Amitay 2002) and substantial drag reductions can be obtained at moderate Reynolds numbers (Amitay *et al.* 1997; Catalano *et al.* 2002).

The objective of this paper is to investigate the accuracy of Reynolds-Averaged Navier-Stokes (RANS) techniques in predicting the effect of steady and unsteady flow control devices. This is part of a larger effort in applying numerical simulation tools to investigate of the performance of synthetic jets in high Reynolds number turbulent flows. RANS techniques have been successful in predicting isolated synthetic jets as reported by Kral *et al.* (1997). Nevertheless, due to the complex, and inherently unsteady nature of the interaction between the synthetic jet and the external boundary layer flow, it is not clear whether RANS models can represent the turbulence statistics correctly.

An extensive computational and experimental investigation of turbulent flow with active control is ongoing at NASA Langley. A workshop, CFDVAL2004, will be held in March 2004 under joint sponsorship by NASA and ERCOFTAC with the objective of providing benchmarks for CFD validation (see `cfdval2004.larc.nasa.gov`). The present work is directed towards participation in this workshop.

† CIRA, Italian Center for Aerospace Research

2. Numerical techniques

2.1. *U-ZEN*

The CIRA U-ZEN code solves the compressible RANS equations around complex aeronautical configurations using multiblock structured grids. The numerical discretization is based on a second-order cell-centered finite-volume method with explicitly added (fourth-order) artificial dissipation. The unsteady solution procedure is based on the dual time stepping method where a pseudo steady-state problem is solved at each time step. Conventional convergence accelerators, including geometrical multigrid and residual smoothing, are used. Several turbulence models are available in U-ZEN: for the numerical simulations presented in this paper only the one-equation Spalart-Allmarass (SA) model (Spalart & Allmaras 1994) and the two-equation k-ω (KW) model (Wilcox 1993) have been used.

2.2. *FLUENT*

FLUENT is a commercial CFD code that solves the RANS equations on hybrid unstructured grids. It uses a second-order upwind discretization based on the SIMPLE pressure-velocity coupling and the formulation can accommodate compressible flows. Dual time stepping is used to obtain time accurate simulations and an algebraic multigrid technique is used to accelerate convergence within each time step. A multitude of turbulence models and variants are available in Fluent. In this work the SA model and Durbin's V2F four-equation model (Durbin 1995) are used. The latter model was implemented in FLUENT using the User Subroutines (Iaccarino 2001).

3. Preliminary validation

As a preliminary step toward applying the two codes to AFC problems, flows around bluff bodies at low Reynolds number are considered. In particular, FLUENT has been successfully applied to compute the vortex shedding in two- and three-dimensional flows (Ooi *et. al.* 2002); the same problems have been carried out using U-ZEN. Only a few results are reported for the flow around the circular cylinder at two Reynolds numbers ($Re_D = 100$ and $Re_D = 3,900$) corresponding to unsteady laminar and turbulent flows. The results are summarized in the Table I.

	U-ZEN	FLUENT	Exp.[1]
St	0.164	0.143	0.165
C_D	1.373	1.377	1.340
C_L	0.292	0.340	0.325
L_R	1.450	1.380	1.460
U_{min}	-0.180	-0.185	-0.180

$Re_D = 100$
[1] Zdravkovich 1997

	U-ZEN	FLUENT	LES[1]	Exp.[2]
St	0.208	0.233	0.203	0.215
C_D	0.865	1.050	1.000	0.980
L_R	1.620	1.360	1.360	1.330
U_{min}	-0.180	-0.185	-0.180	-0.180

$Re_D = 3,900$
[1] Beaudan & Moin 1994, [2] Zdravkovich 1997

Table I. Computational results for the flow around the circular cylinder. St is the Strouhal number, C_D and C_L are the maximum aerodynamic forces during a shedding cycle, L_R the length of the recirculation bubble, and U_{min} the minimum velocity on the wake centerline.
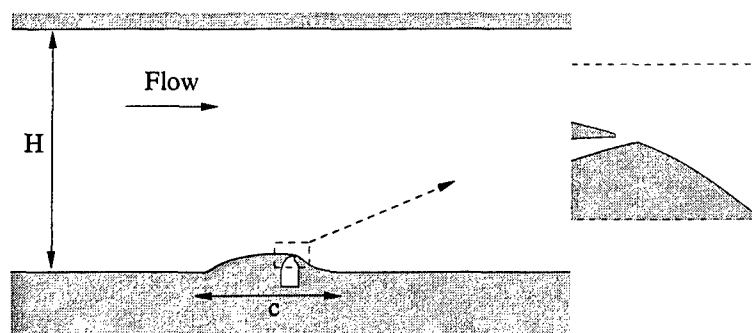
FIGURE 1. Sketch of the bump studied experimentally by Seifert & Pack (2002)

U-ZEN and FLUENT are in good agreement with each other and with the experimental data. Additional simulations were carried out for the flow over a square cylinder, and similar agreement was obtained.

4. Turbulent flow over a bump

Three problems have been proposed for the CFDVAL2004 Workshop: the first two are related to simple synthetic jet flows with and without crossflow. The third concerns the study of a hump model with various steady and unsteady separation controls. Our preliminary work has been focused on the analysis of this test problem.

The geometry with a detailed view of the flow control slot is sketched in Fig. 1. The hump thickness is 20% and the chord of the hump relative to to the height of the channel is $c/H = 2/3$ and, therefore, substantial blockage effects are expected.

Experiments were carried out in the NASA Langley Transonic Cryogenic Tunnel (Seifert & Pack 2002) for Reynolds numbers ranging from 2.4 to 26 millions and Mach number of 0.25. Due to discrepancies observed with previous CFD analysis of this model (see Viken *et. al.* 2003) a new set of measurements will be collected and made available at the workshop. In this work we will the original set of experimental data for an initial assessment of the predictive capabilities of the RANS tools employed.

Structured and unstructured computational grids have been generated. The unstructured grid (Fig. 2) is built using 24 layers of quadrilaterals in the boundary layers and paving in the rest of the domain. Three meshes were considered to evaluate the grid sensitivity of the solution; their sizes range from 12,000 to 70,000 elements. Note that the cavity region is included in the mesh (using triangular paving) to study its effect on the solution. The structured grid is shown in Fig. 3. It contains 16,000 cells, and two additional coarser versions have been considered to evaluate grid dependence. In this case the cavity is not included and the jet control is modeled through a boundary condition to be discussed later.

The first set of simulations is aimed at establishing the accuracy of the two RANS codes used (UZEN and FLUENT) for a case without flow control. Calculations are carried out at Reynolds number of 12 million and Mach 0.25. In Fig. 4 pressure coefficient distributions along the bump are reported using various turbulence models and by considering different heights of the channel to study the effect of the blockage. The agreement is reasonable when the SA and KW models are used in FLUENT and UZEN, respectively. When the same turbulence model (SA) is used the comparison is not satisfactory, with UZEN predicting a substantially lower pressure. The cause seems to be related to the
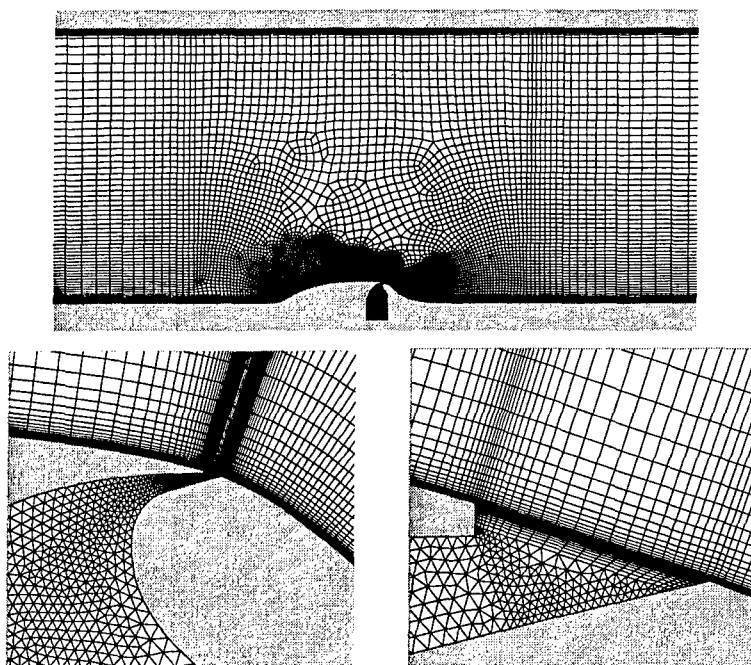
FIGURE 2. Unstructured computational grid with details of the slot region.
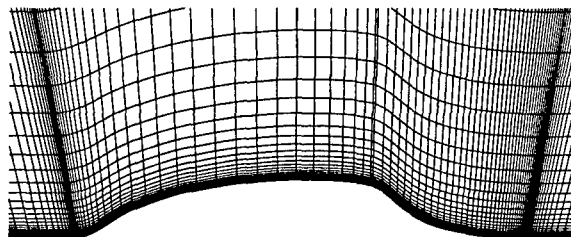

FIGURE 3. Structured computational grid. Note that the cavity is not included but is modeled as a boundary condition.

incoming boundary layer (note the peak at $x/c = 0$ in Fig. 4(a)) which appears to be of different thickness in the various calculations. This was also acknowledged as a crucial aspect of the simulations reported in Viken et. al. (2003).

The effect of the blockage plotted in Fig. 4(b) shows that the separation bubble (from $x/c \approx 0.6$) is strongly affected by the height of the channel; however, the simulations fail to capture the level of the pressure in the separated region. This is consistent with the finding in Viken et. al. (2003) which has motivated the new experimental study.

In Fig. 5 the streamlines are reported for the cases without control and with a steady suction corresponding to a momentum coefficient $C_\mu = -1.4\%$ (where C_μ is defined as the ratio of jet momentum to free-stream momentum). The recirculation bubble in Fig. 5(a), estimated using the skin friction coefficient (not reported), is $\Delta/c = 0.59$ whereas it is reduced to $\Delta/c = 0.14$ with the control (Fig. 5(c)). The experimental bubble length
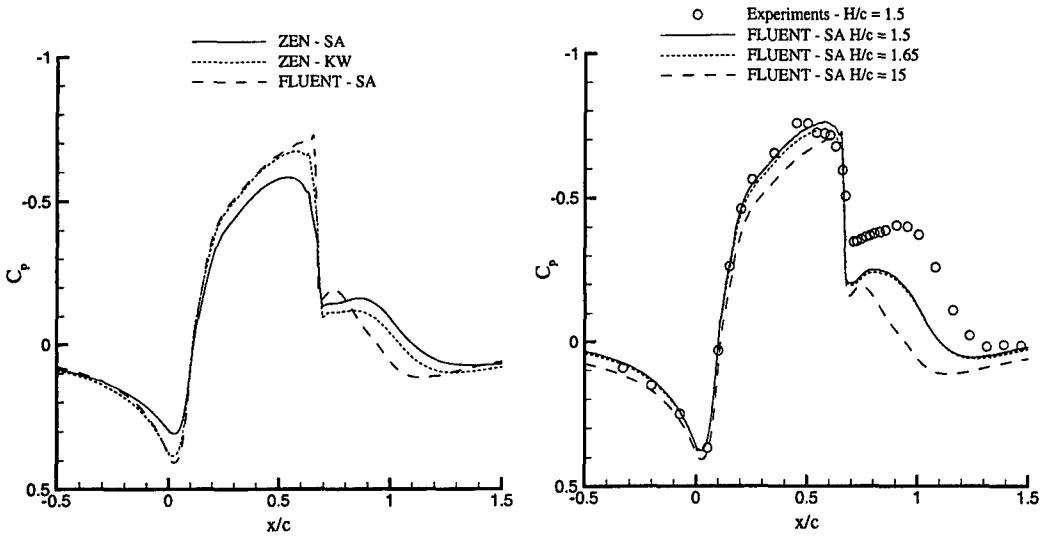
FIGURE 4. Pressure coefficient distribution over the bump; Re = 16 million, Ma = 0.25. Comparison between U-ZEN and FLUENT (left); effect of the height of the tunnel (right), cfn. Fig. 1.
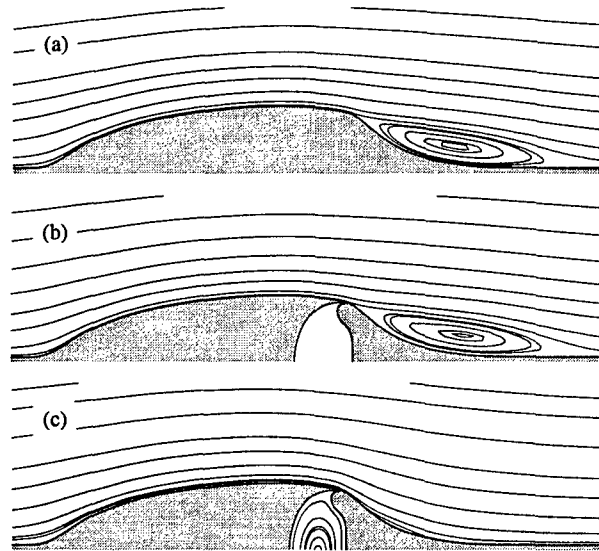

FIGURE 5. Computed streamlines: Re = 16 million, Ma = 0.25. No control (left); no control but model with the cavity (center), steady suction: $C_\mu = -1.4\%$ (right).

is estimated to be $\Delta/c = 0.56$ for the case without control. No information is given for the case with control in Seifert & Pack (2002). In Fig. 5(b) an additional simulation is reported for the case without control but with the cavity to evaluate its effect on the solution.

One important aspect of the present work is to establish the suitability of representing the control jets using boundary conditions instead of explicitly simulating the flow in the
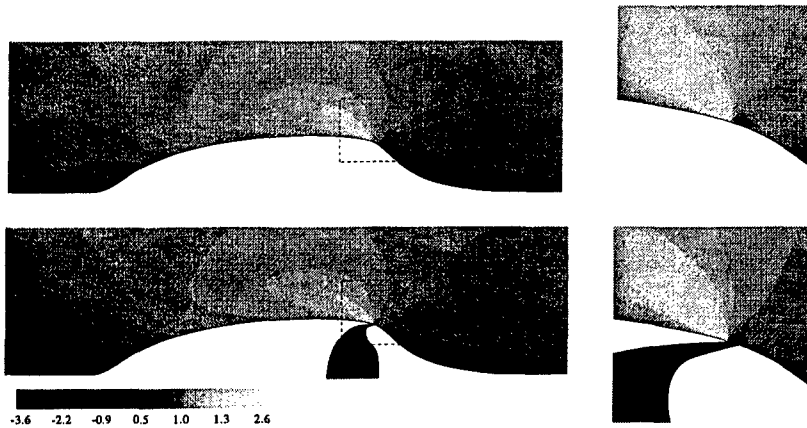
-3.6   -2.2   -0.9   0.5   1.0   1.3   2.6

FIGURE 6. Computed streamwise velocity contours. Steady suction modeled as a boundary condition (top) and steady suction applied through the cavity (bottom).

cavity. This is extremely important for synthetic jets generated by a deforming membrane which would require an extremely complicated and time-consuming moving-mesh calculation. In Fig. 6 two simulations of the steady suction control case (reported earlier) are compared. In one case the suction is modeled as a boundary condition whereas in the other the cavity is included in the simulation. From an experimental point of view the momentum ratio C_μ is known together with the total mass flow rate through the slot:

$$C_\mu = \frac{\rho_j V_j^2 H}{1/2 \rho_\infty V_\infty^2 c}$$
$$M_j = \frac{\rho_j V_j H}{\rho_\infty V_\infty c}$$

where the subscripts j and ∞ refer to jet and inflow conditions, respectively, and M_j is the measured mass flow through the slot. These two conditions allow the jet conditions to be determined:

$$\frac{V_j}{V_\infty} = \frac{C_\mu}{2M_j}$$
$$\frac{\rho_j}{\rho_\infty} = \frac{V_\infty}{V_j} \frac{M_f c}{H}$$

The suction boundary condition is formulated by assuming a constant density and velocity (given by the expressions above) and by assuming a zero pressure gradient. The results are presented in Fig. 6 in terms of velocity contours on the bump and in the vicinity of the suction slot. The agreement between the two simulations (with the cavity or with the suction boundary condition) is very good. Another option that has been tested for the specification of the boundary condition is to use a zero gradient condition for the velocity corresponding to an extrapolation from the inside (instead of a direct enforcement). This condition will not guarantee the correct specification of the mass flow and, therefore, the velocity has to be properly scaled. The advantage of this approach is that the velocity is not constant in the slot region but has a variation that accounts
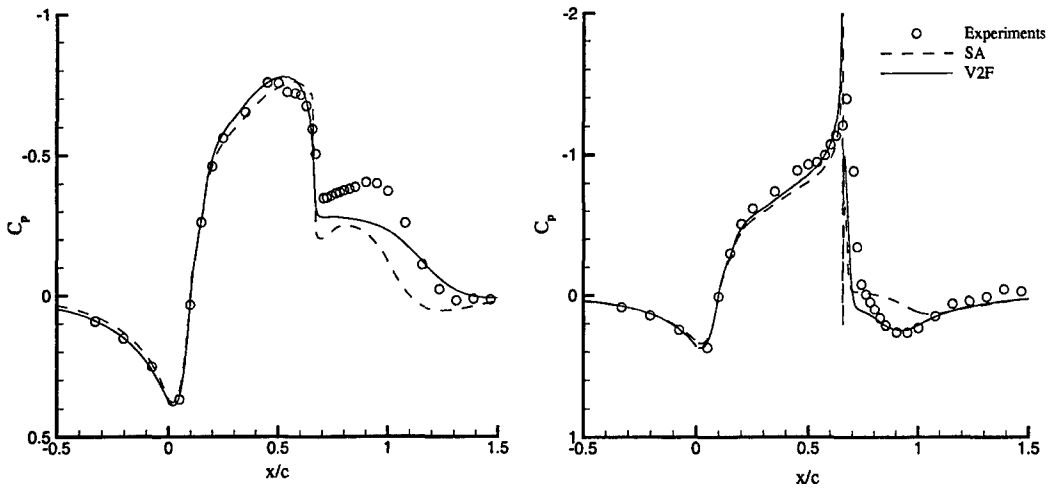
FIGURE 7. Pressure coefficient distribution over the bump: Re = 16 million, Ma = 0.25. No control (left); steady suction: $C_\mu = -1.4\%$ (right).

for the external flow even if the correct suction integral parameters are specified. The difference between the two boundary conditions described was found to be minimal in the present problem.

In Fig. 7 the pressure distributions on the bump with and without (steady) control are reported. Results obtained using two turbulence models are compared with the experimental data. The V2F model appears to be superior to the SA model in predicting the pressure level in the recirculation bubble and in the successive recovery region (as expected, see Iaccarino 2001). In particular, it is interesting to note that the agreement is somewhat better in the controlled case.

Finally, in Fig. 8, results for an unsteady control case are reported. They correspond to an average momentum coefficient $< C_\mu > = 0.95\%$ and a non-dimensional frequency $F^+ = 1.6$ (normalized by free stream velocity and half chord). In this case experimental data are not available for comparison, but the present data are is agreement with the CFD results reported in Viken *et. al.* (2003). It is interesting to note that the envelope (the maximum and minimum within a cycle) shows a large variation of the friction coefficient in the region downstream of the slot with a very small area of recirculating flow.

5. Conclusions and future work

This report presents some preliminary results of steady and unsteady RANS simulations of flows with active control. The main objective is to establish the accuracy of the predictions with particular emphasis on (a) turbulence modeling, and (b) control enforcement (boundary condition).

Calculations are carried out using an unstructured commercial CFD code, FLUENT, and a multiblock structured aeronautical CFD code, UZEN. Several turbulence model have been used, ranging from a one-equation model to a four-equation model. An explicit description of the control device (a cavity with a contoured slot) and its modeling by a velocity boundary condition have been considered and results have been compared.
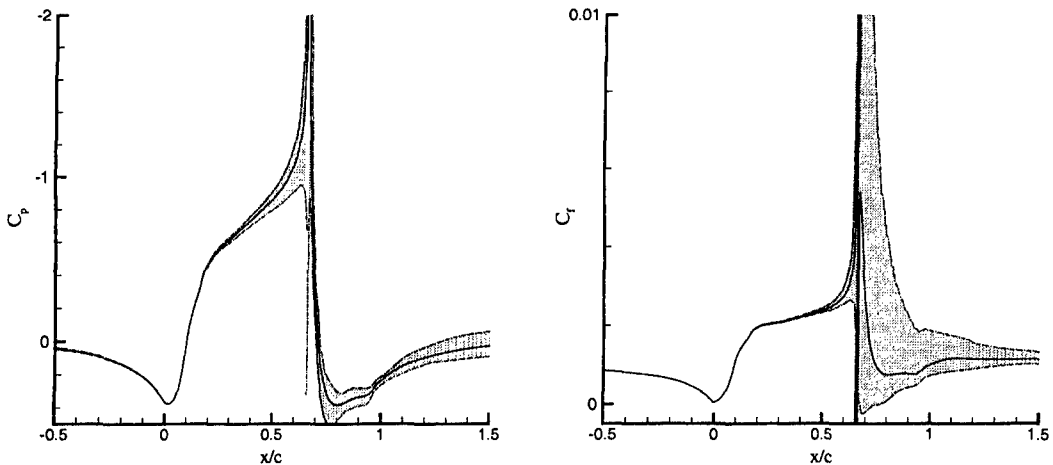
FIGURE 8. Pressure coefficient distribution (left) and skin friction (right) over the bump in the unsteady control case: Re = 16 million, Ma = 0.25. Solid line represent time averaged results; the grey area represents the unsteady envelope. These results are obtained with the full configuration (including the cavity).

The preliminary conclusion is that turbulence modeling plays a crucial role in the accuracy of the results and, at least for a steady suction control, the control device can be reasonably modeled by a boundary condition.

Future work will be focused on the comparison of the present calculation (and additional simulations in different conditions) to the new set of experimental data being provided at the CFDVAL2004 workshop and on the assessment of the suitability of modeling unsteady control (synthetic jet) by boundary conditions.

REFERENCES

AMITAY, M., SMITH, B.L. & GLEZER, A. 1997 Modification of the aerodynamic characteristics of bluff bodies using fluidic actuators. *AIAA Paper 97-2004* .

BEAUDAN, P. & MOIN, P. 1994 Numerical experiments of the flow past a circular cylinder at subcritical Reynolds number. *Rept. No. TF-62, Dept. Mech. Eng.* Stanford University.

BRASLOW, A. L. 1999 *A history of suction-type laminar flow control with emphasis on flight research.* NASA Monographs **13**.

CATALANO, P., WANG, M., IACCARINO, G., SBALZARINI, L. & KOUMOUTSAHOS, P. 2002 Optimization of cylinder flow control via actuators with zero-mass flux. *Proc. of the 2002 Summer Program*, Center for Turbulence Research, 297–304.

DURBIN, P. A., 1995 Separated flow computations with the $k - \epsilon - v^2$ model. *AIAA J.*, **33**, 659–664.

GLEZER, A. & AMITAY, M., 2002 Synthetic jets. *Ann. Rev. Fluid. Mech.* **34** 503–529.

IACCARINO, G., 2001 Predictions of a turbulent separated flow using commercial CFD codes. *J. Fluids Eng.* **123** 819–828.

KRAL, L. D. , DONOVAN, J. F., CAIN, A. B. & CARY, A. W. 1997 Numerical simulation of synthetic jet actuators. *AIAA Paper 97-1824* .

OOI, A., IACCARINO, G., DURBIN, P. A. & BEHNIA, M., 2002 Reynolds averaged simulations of flow and heat transfer in ribbed ducts. *Int. J. Heat and Fluid Flow*, **23**, 750–757.

SEIFERT, A. & PACK, L. G., 2003 Active flow control on wall-mounted hump at high Reynolds numbers. *AIAA J.* **40** 1363–1372.

SMITH, B. L. & SWIFT, G. W., 2003 A comparison between synthetic jets and continuous jets. *Exp. Fluids* . **34** 467–472.

SPALART, P. R. & ALLMARASS S. R., 1994 A one-equation turbulence model for aerodynamic flows. *La Recherche Aerospatiale*, **1**, 1–23.

VIKEN, S. A., VATSA, V. N., RUMSEY, C. L. & CARPENTER, M. H., 2003 Flow control analysis of the hump model with RANS tools. *AIAA Paper 2003-218*

WILCOX D.C. 1993 *Turbulence modeling for CFD*. DCW Industries Inc., USA.

ZDRAVKOVICH, M. M. 1997 *Flow Around Circular Cylinders. Fundamentals.* Oxford University Press, Oxford, UK.